

Published in final edited form as:

Nat Immunol. 2014 October ; 15(10): 965–972. doi:10.1038/ni.2981.

AMPK-TAB1 activated p38 drives human T cell senescence

Alessio Lanna¹, Sian M. Henson¹, David Escors^{1,2}, and Arne N. Akbar^{1,†}

¹Division of Infection and Immunity, The Rayne Building, University College London, London, United Kingdom

²Navarrabiomed-Fundacion Miguel Servet, Calle Irunlarrea n 3, Complejo Hospitalario de Navarra, 31008. Pamplona, Navarra. Spain

Abstract

In T lymphocytes, p38 MAP kinase (MAPK) regulates pleiotropic functions and is activated by canonical MAPK signaling or the alternative T cell receptor (TCR) activation pathway. Here we show that senescent human T cells lack the canonical and alternative pathways of p38 activation, but spontaneously engage the metabolic master regulator AMPK to trigger p38 recruitment to the scaffold TAB1 causing p38 auto-phosphorylation. Signaling via this pathway inhibits telomerase activity, T cell proliferation and expression of key components of the TCR signalosome. Our findings identify an unrecognized mode of p38 activation in T cells driven by intracellular changes such as low-nutrient and DNA-damage signaling ('intra-sensory' pathway). The proliferative defect of senescent T cells is reversed by blocking AMPK-TAB1-dependent p38 activation.

Introduction

T cell proliferative responses are essential for the lifelong preservation of adaptive immunity. Optimal T cell activation requires both T cell receptor (TCR) engagement and co-stimulatory signals¹ however progressive loss of CD27 and CD28 co-stimulatory receptors occurs during end-stage T cell differentiation towards senescence that correlates well with a loss of proliferation². The mechanisms that regulate the loss of proliferative potential in highly differentiated T cells are poorly understood. The aim of this study is to identify mechanisms involved in human end-stage T cell differentiation and whether intervention is possible to restore proliferative activity in these cells.

The loss of surface CD27, followed by loss of CD28 expression during human CD4⁺ T cell differentiation³ enables the identification of undifferentiated T cells that have high proliferative activity and the longest telomeres (CD27⁺ CD28⁺); intermediate differentiated cells that have reduced proliferation and telomeres of intermediate length (CD27⁻ CD28⁺) and end-stage or senescent T cells that proliferate poorly and have the shortest telomeres

Users may view, print, copy, and download text and data-mine the content in such documents, for the purposes of academic research, subject always to the full Conditions of use:http://www.nature.com/authors/editorial_policies/license.html#terms

†Corresponding author: Professor Arne N. Akbar, Division of Infection and Immunity, University College London, 5 University Street, London, WC1E 6JF, UK a.akbar@ucl.ac.uk.

Contributions: A.L. conceived of, designed and did the study, analyzed and interpreted all data and wrote the paper. S.M.H. did experiments. D.E provided lentiviral tools. A.N.A. wrote the paper and provided overall direction. All authors read and approved the final version of the manuscript.

(CD27⁻ CD28⁻)³. Senescent CD27⁻ CD28⁻ CD4⁺ T lymphocytes accumulate significantly in old humans, in patients with chronic viral infections and in those with autoimmune disorders³⁻⁷. The senescence characteristics of these cells include short telomeres, low telomerase activity and reduced proliferative capability⁸ that is due in part to a spontaneous but unexplained increase in p38 MAPK activity⁹. Nevertheless CD27⁻ CD28⁻ CD4⁺ T cells exhibit potent effector functions and cannot be viewed as a dysfunctional population *per se*³⁻⁷. Here we investigated the regulatory network upstream of p38 MAPK in the senescent CD27⁻ CD28⁻ CD4⁺ T cell subset. The p38 MAPK family comprises α , β , γ and δ isoforms that regulate a number of different functions in a cell-type and stimulus dependent manner¹⁰. T lymphocytes mainly express the α and to a lesser extent the β and δ isoforms of p38¹⁰. The canonical MAPK cascade is the main mechanism for activation of all four p38 isoforms in mammalian cells, including T cells¹⁰⁻¹². Signaling through the MAPK pathway activates p38 by dual phosphorylation on Thr¹⁸⁰ and Tyr¹⁸² sites in response to environmental stress, inflammation, DNA damage¹² and also co-stimulatory receptor engagement¹³. In addition, T cells have an alternative pathway of p38 activation, in which antigenic stimulation via the T cell receptor (TCR) induces p38 α and β phosphorylation on Tyr³²³ by TCR-proximal tyrosine kinases¹⁴, followed by auto-phosphorylation on Thr¹⁸⁰ and Tyr¹⁸² (14).

We now demonstrate that instead of using the canonical or the alternative pathways, freshly isolated CD27⁻ CD28⁻ CD4⁺ T lymphocytes engage a distinct mechanism whereby the intracellular metabolic sensor AMPK triggers p38 auto-phosphorylation via the scaffold protein TAB1. Furthermore, signaling through this pathway down-regulates central components of the TCR signalosome, a previously unidentified characteristic of T cell senescence. Activation of p38 through AMPK-TAB1 can be induced by both endogenous DNA damage but also by a fall of intracellular energy levels. Thus, unlike the canonical and alternative pathways for p38 activation that respond to external cues (e.g. cytokines or TCR activation), T cells have an ‘intra-sensory’ pathway for p38 activation that senses intracellular changes such as glucose deprivation and genotoxic stress. Once triggered, this pathway inhibits T cell proliferation and telomerase activation via p38 MAPK signaling and this can be reversed by inhibiting AMPK, TAB1 or p38 itself.

Results

p38 activation in the absence of canonical and alternative pathways

The relative expression of CD27 and CD28 receptors identifies three distinct populations in primary human CD4⁺ T cells (Fig. 1a). CD27⁻ CD28⁻ T cells are known to exhibit low telomerase and proliferative activity upon activation³, which are characteristics of end-stage differentiation or senescence^{3, 4, 9, 15}. The CD27⁻ CD28⁻ subset of CD4⁺ T cells also exhibits endogenously elevated p38 (Thr¹⁸⁰ and Tyr¹⁸²) phosphorylation that is significantly higher than CD27⁺ CD28⁺ or CD27⁻ CD28⁺ T cell subsets *in vivo* (by 2-2.5 fold, $p < 0.001$; Fig. 1b).

We investigated whether the canonical MAPK cascade, which regulates p38 activation in response to stress stimuli and co-stimulatory receptor engagement^{12, 13} was responsible for the endogenous p38 activation observed in CD27⁻ CD28⁻ CD4⁺ T cells. Freshly isolated human CD27⁻ CD28⁻ CD4⁺ T cells did not express nor activate either MKK3 or MKK6

(Fig. 1c,d), the direct upstream regulators of p38 in this signaling cascade¹². Similarly, these cells did not activate MKK4 (data not shown), an activator of the MAP kinase JNK¹⁶ which in some instances may also activate p38 (ref 10). Furthermore, phorbol 12-myristate 13-acetate (PMA), a well-established agonist of canonical MAPK cascade¹⁷, failed to enhance p38 activity in CD27⁻ CD28⁻ CD4⁺ T cells, while inducing a significant increase of p38 phosphorylation in the undifferentiated CD27⁺ CD28⁺ subset ($p < 0.001$; Fig. 1e,f). Similar observations were made when inducing the p38 canonical pathway by an osmotic stressor (sorbitol, data not shown). Thus, despite the constitutive increase in p38 activity (Fig. 1b), human senescent CD27⁻ CD28⁻ CD4⁺ T cells do not regulate p38 signaling by the canonical MAPK cascade.

Antigenic stimulation through the TCR activates p38 by an alternative pathway where a protein tyrosine kinase (PTK) cascade that is dependent on LCK and mediated by ZAP-70, phosphorylates p38 at Tyr³²³ (ref 14). The membrane-associated scaffold molecule DLG1 binds p38 and coordinates this process¹⁸. Because persistent antigenic stimulation drives human T cell differentiation *in vivo*^{2, 3}, we tested if the alternative pathway of p38 activation through TCR signaling was responsible for inducing p38 signaling in CD27⁻ CD28⁻ CD4⁺ T cells. However, we found that the CD27⁻ CD28⁻ CD4⁺ population did not phosphorylate p38 on the alternative Tyr³²³ site either before or after anti-(α)CD3 stimulation (Fig. 1g). In contrast, undifferentiated CD27⁺ CD28⁺ CD4⁺ T cells expressed high levels of phosphorylated p38 (Tyr³²³) upon CD3 activation (Fig. 1g).

We next investigated the expression of the elements of the TCR signalosome that constitute the alternative pathway of p38 activation in CD27⁺ CD28⁺, CD27⁻ CD28⁺ and CD27⁻ CD28⁻ CD4⁺ T cells. We found that freshly isolated CD27⁻ CD28⁻ CD4⁺ T cells did not express Lck, Zap70 and DLG1 in contrast to the CD27⁺ CD28⁺ and CD27⁻ CD28⁺ CD4⁺ subsets (Fig. 1h,i). In addition, these cells also lacked other essential downstream components of the TCR signaling machinery, such as the adaptors Lat and SLP-76 and had very low expression of the phospholipase PLC- γ 1 (Supplementary Fig. 1a,b). The loss of TCR signaling machinery in senescent CD27⁻ CD28⁻ CD4⁺ T cells was also associated with defective calcium influx upon α CD3 stimulation, indicating that the loss of TCR signaling molecules impaired TCR responsiveness (Supplementary Fig. 1c,d). Taken together, these data indicate that the spontaneous increase of p38 activity observed in CD27⁻ CD28⁻ CD4⁺ T cells is not regulated by either the canonical MKK or alternative TCR mediated signaling pathways, in contrast to p38 regulation in non-senescent CD4⁺ T cells^{11, 19}.

p38 activation is triggered by AMPK and mediated by TAB1

In human embryonic kidney (HEK) 293-cells, allosteric p38 (Thr¹⁸⁰ and Tyr¹⁸²) auto-phosphorylation is induced independently of upstream MKKs via the scaffold molecule TAB1²⁰. We investigated whether TAB1 signaling was involved in the constitutive p38 activation observed in senescent CD27⁻ CD28⁻ CD4⁺ T cells. Two TAB1 splicing-variants (α or β), of 60-kDa and 50-kDa, bind to and activate p38 by an identical mechanism²¹. Using a monoclonal antibody directed against the p38-binding domain common to both isoforms, we found that CD27⁻ CD28⁻ CD4⁺ T cells expressed the 50-kDa isoform of

TAB1 (Fig. 2a), which does not bind to nor regulate TAK1²¹. In addition CD27⁻ CD28⁻ CD4⁺ T cells also did not express TAK1 itself (Fig. 2a). Conversely, non-senescent T cell subsets expressed TAK1 and also the full length TAB1, which binds to TAK1 (Fig. 2a). Because the activation of the TAB1 pathway requires non-degradative ubiquitination by the upstream E3 ubiquitin-ligase TRAF6²⁰, we examined the expression of TRAF6 in the non-senescent and senescent CD4⁺ T cell subsets. CD27⁻ CD28⁻ CD4⁺ T cells lacked TRAF6 expression (Fig 2a), indicating that the TRAF6-TAK1 pathway is not active in these cells.

AMPK, is activated in response to low intracellular levels of glucose and has been shown to bind to TAB1 in mouse ischemic cardiomyocytes²². This molecule is activated by phosphorylation on Thr¹⁷² in its catalytic α -subunit to shift metabolism towards catabolic reactions²³. In addition, AMPK inhibits mTOR activity in T cells^{24,25}. We investigated whether AMPK regulates p38 activity in CD27⁻ CD28⁻ CD4⁺ T cells through TAB1. Freshly isolated human CD27⁺ CD28⁺, CD27⁻ CD28⁺ and CD27⁻ CD28⁻ CD4⁺ T cells all expressed AMPK α , but only the CD27⁻ CD28⁻ CD4⁺ T cell subset showed spontaneous AMPK α activation (p-AMPK α ; Fig. 2b). To determine whether AMPK was acting upstream of p38 in T cells, we treated CD27⁺ CD28⁺ CD4⁺ T cells, that have no base-line AMPK activity (Fig. 2b) and exhibit low spontaneous p38 phosphorylation (Fig. 1b), with the selective AMPK agonist A-769662²⁶. The agonist induced significant p38 (Thr¹⁸⁰ and Tyr¹⁸²) phosphorylation in CD27⁺ CD28⁺ CD4⁺ T cells ($p < 0.01$; Fig. 2c,d). Despite their high baseline p38 activity, A-769662 also enhanced p38 (Thr¹⁸⁰/Tyr¹⁸²) phosphorylation in senescent CD27⁻ CD28⁻ CD4⁺ T cells (data not shown).

To directly investigate the role of TAB1 and AMPK signaling on p38 activation, we used VSV-g pseudo-typed lentiviral vectors co-expressing a GFP reporter gene and short-hairpin (sh) RNAs silencing either the catalytic α subunit of AMPK (shAMPK α) or a region common to both the 60 and 50-kDa isoforms of TAB1 (shTAB1) (Supplementary Fig. 2a-d). An irrelevant, scrambled hairpin expressing vector (shCtrl) was used as control (Supplementary Fig. 2c,d). Isolated CD27⁻ CD28⁻ CD4⁺ T cells were transduced with these vectors 48 hours after activation with α CD3 and rh-IL-2. Four days post-transduction, we examined changes in p38 phosphorylation (Thr¹⁸⁰ and Tyr¹⁸²) in GFP⁺ T cells by phospho-flow analysis (Fig. 2e). Under steady-state conditions, both AMPK α and TAB1-silenced GFP⁺ T cells showed a significant inhibition of p38 activity compared to scrambled control vector ($p < 0.01$; Fig. 2e), indicating that AMPK and TAB1 regulate p38 activation in human senescent CD4⁺ T cells.

We next treated the shAMPK α transduced CD27⁻ CD28⁻ CD4⁺ T cells with the AMPK agonist A-769662 for 1 hour followed immediately by phospho-flow analysis of p38 activation in the GFP⁺ T cells (Fig. 2f,g). The AMPK agonist-induced activation of p38 was inhibited in the CD27⁻ CD28⁻ CD4⁺ T cells confirming that the process was AMPK dependent (Fig. 2f,g). The AMPK agonist-induced p38 activation was also inhibited in TAB1-silenced CD4⁺ CD27⁻ CD28⁻ T cells (Fig. 2h,i), indicating that AMPK requires TAB1 to activate p38 in these cells. Silencing of either AMPK α or TAB1 in AMPK agonist-activated CD27⁻ CD28⁻ CD4⁺ T cells also inhibited phosphorylation of the p38 substrate ATF2 (at residue Thr⁷¹) (Fig. 2h,i). Similarly, agonist-driven AMPK activation failed to activate p38 in AMPK and TAB1-silenced CD27⁺ CD28⁺ CD4⁺ T cells (data not shown).

Thus, AMPK activation induces p38 MAPK signaling in a TAB1-dependent way in senescent human CD4⁺ T cells.

DNA damage and low-nutrient sensing by AMPK activates p38

Cellular AMPK is mainly activated in response to decreased intracellular ATP²³. However, we did not find a reduction of cellular ATP levels in freshly isolated senescent human CD27⁻ CD28⁻ CD4⁺ T cells compared to the CD27⁺ CD28⁺ and CD27⁺ CD28⁻ subsets (data not shown). Because only end-stage differentiated CD27⁻ CD28⁻ CD4⁺ T cells exhibited spontaneous AMPK activity, we investigated whether various end-stage differentiation features of these cells triggered AMPK activation. We found evidence of endogenous DNA damage²⁷ in CD27⁻ CD28⁻ CD4⁺ T cells, including spontaneous phosphorylation of the DDR apical kinase ATM (Ser¹⁹²¹) (Fig. 3a,b) and of its downstream target H2A-X (Ser¹³⁹) (Fig. 3c,d), which have been previously used as indicators of active DNA damage foci²⁸. Inhibition of ATM activity by the selective ATM inhibitor KU-55933 for 1 hour inhibited constitutive AMPK α (Thr¹⁷²) and p38 (Thr¹⁸⁰-Tyr¹⁸²) phosphorylation in CD27⁻ CD28⁻ CD4⁺ T cells (Fig. 3e-h), indicating that ATM acted 'upstream' of both molecules in these cells. We also found elevated reactive oxidative species (ROS) expression in these cells (Supplementary Fig. 3a). Because genotoxic stress by ROS induces DNA damage²⁹ and because ROS are a known activator of AMPK³⁰, we tested the effect of the ROS scavenger superoxide-dismutase (SOD) on ATM, AMPK and p38 activation. ROS scavenging impaired activation of all three molecules in CD27⁻ CD28⁻ CD4⁺ T cells (Supplementary Fig. 3b,c), suggesting that ROS may be triggering the endogenous DNA damage response leading to p38 activation in human senescent T cells.

Because AMPK acts as a low-glucose sensor in cells^{23, 24}, we tested if glucose deprivation also induced AMPK-dependent p38 activation in non-senescent T cells that have intact DNA and low ROS production (Fig. 3a-d and Supplementary Fig. 3a). Glucose starvation of undifferentiated CD27⁺ CD28⁺ CD4⁺ T cells enhanced p38 phosphorylation (Fig. 3i,j). Silencing of either AMPK or TAB1 effectively inhibited p38 phosphorylation following glucose deprivation in these cells compared to scrambled control transduced cells (Fig. 3k,l). Taken together, these data support a model where signals from both genotoxic and nutrient sensing pathways converge at the point of AMPK in T cells, which subsequently activates p38 through the scaffold molecule TAB1.

AMPK triggered p38 recruitment to TAB1 causes p38 auto-phosphorylation

To further dissect the mechanistic details of the AMPK-TAB1-p38 pathway, we performed immunoprecipitation studies in primary human CD27⁺ CD28⁺ CD4⁺ T cells activated by the AMPK agonist (A-769662). Immunoblot analysis of TAB1 immunoprecipitates from these cells showed that agonist-driven AMPK activation promoted p38 recruitment to TAB1 (by 2.5-3 fold, Fig. 4a,b). Furthermore, TAB1 immunoprecipitates were specifically enriched for both phosphorylated AMPK and p38 (Fig. 4a), suggesting the existence of an active AMPK-TAB1-p38 complex. Similarly, TAB1 immunoprecipitates from glucose-starved undifferentiated CD27⁺ CD28⁺ CD4⁺ T cells were also enriched for both phosphorylated AMPK and p38 (data not shown). Importantly, activated AMPK and p38 were constitutively present in TAB1 immunoprecipitates from CD27⁻ CD28⁻ CD4⁺ T cells (Fig. 4c), in which

the AMPK-TAB1-p38 pathway is constitutively active (see above). Because TAB1 mediates p38 auto-phosphorylation²⁰ (a modification that relies on the intrinsic activity of the kinase) and because p38 is not a direct substrate for AMPK, these data suggested that AMPK may induce p38 auto-phosphorylation via eliciting its binding to TAB1.

We therefore immunoprecipitated p38 from AMPK agonist-activated CD27⁺ CD28⁺ CD4⁺ T cells that were transduced with either shTAB1 or shAMPK α and assessed the kinase activity of p38 in the absence of an added substrate *in vitro* (e.g. to determine p38 auto-phosphorylation^{14, 18}). Using this assay, we detected activated p38 in immunoprecipitates from scrambled control-transduced CD27⁺ CD28⁺ CD4⁺ T cells, and this activity was enhanced by the addition of ATP *in vitro*. Conversely, adding ATP to p38 immunoprecipitates from shTAB1 or shAMPK α -transduced CD27⁺ CD28⁺ CD4⁺ T cells did not increase p38 activity *in vitro* (Fig. 4d). This indicates that p38 auto-phosphorylation requires both AMPK-TAB1 with which p38 interacts in response to AMPK activation.

To confirm that the above experiment was indicative of p38 auto-phosphorylation (and not an event mediated by an unrelated co-immunoprecipitated kinase), we added the ATP-competitor SB-203580, which acts as an inhibitor of p38, directly to the *in vitro* kinase reaction itself. SB-203580 prevented the enhanced p38 phosphorylation *in vitro* in response to exogenous ATP (but not the baseline kinase activation within the cells) in TAB1 immunoprecipitates after AMPK activation (Fig. 4e). Similar results were obtained with a different inhibitor of p38 activity (BIRB 796, data not shown). Thus, the p38 recruited at the AMPK-TAB1 complex auto-phosphorylates.

AMPK or TAB1 silencing restores proliferation in senescent T cells

Loss of telomerase activity in senescent T cells^{3, 8, 15} limits their proliferative potential after antigenic challenge both *in vitro* and *in vivo*^{31, 32} and is mediated in part by p38 activation, as shown by rescue with a selective p38 small molecule inhibitor^{9, 33}. To test whether TAB1 or AMPK α silencing restored these functions in senescent T cells, we transduced activated, purified CD27⁻ CD28⁻ CD4⁺ T cells with the shAMPK α and shTAB1 lentiviral vectors (Supplementary Fig. 4a). Because telomerase activity in T lymphocytes specifically requires re-expression of the related catalytic subunit (hTERT) upon activation³⁴, we measured hTERT expression by both immunoblot and quantitative PCR. hTERT expression was significantly enhanced in both AMPK α and TAB1-silenced CD27⁻ CD28⁻ CD4⁺ T cells compared to scrambled control-transduced cells, one week after activation with anti-CD3 and rh-IL-2 ($p < 0,01$; Fig. 5a), leading to increased telomerase activity in these cells at the one week time point, as assessed by TRAP assay (Fig. 5b).

To assess the *in vivo* effect of enhanced telomerase activity in TAB1- or AMPK α - silenced CD27⁻ CD28⁻ CD4⁺ T cells, we measured telomere length by fluorescence *in situ* hybridization coupled to flow cytometry (flow-FISH), as described¹⁵. Four weeks after lentiviral vector transduction (Supplementary Fig. 4a), TAB1 or AMPK α knockdown induced a significant extension (0.5-0.7 kb) of telomeric length in the GFP⁺ CD27⁻ CD28⁻ CD4⁺ T cells compared to scrambled control cells ($p < 0.001$; Fig. 5c,d). Furthermore, the silencing of either TAB1 or AMPK α significantly enhanced the short-term proliferation of CD27⁻ CD28⁻ CD4⁺ T cells following activation with anti-CD3 and rh-IL-2 for 7 days, as

assessed by either thymidine incorporation (to assess *de novo* DNA synthesis) or dye dilution analysis ($p < 0.01$; Fig. 5e,f,g) as well as their long-term expansion capacity (30 days in culture) compared to scrambled control (Fig. 5h). As a control, inhibition of p38 by shP38 or by blocking with two different specific inhibitors (BIRB 796 or SB203580) resulted in enhanced telomerase activity and short and long-term proliferation of senescent T cells (Supplementary Fig. 4b-g and data not shown), confirming previous studies⁹. Thus, the defective proliferation and telomerase activity of human senescent T cells can be reversed by the inhibition of AMPK and TAB1 upstream of p38.

To further dissect the role of p38 activation in the proliferation of human senescent T cells, we investigated the impact of p38 on the cell-cycle machinery. Because p38 blockade increased the rate of DNA synthesis (an event that characterizes actively S-phase cycling cells), we investigated the expression of several G1/S transition regulators in CD27⁻ CD28⁻ CD4⁺ T cells activated with anti-CD3 and rh-IL-2. Inhibition of p38 induced the coordinated down-modulation of cell-cycle inhibitors (p27, p21), up-regulation of D cyclins, enhanced Rb inactivation (by lowering the expression of active, under-phosphorylated Rb) and dampened activation of the tumour suppressor p53 that are all well-established events that promote the G1/S transition³⁵ (Supplementary Fig. 5 and data not shown). Similar results were also obtained when tuning p38 activity by silencing AMPK or TAB1 with shRNAs in CD27⁻ CD28⁻ CD4⁺ T cells (data not shown), indicating that p38 activation induced by AMPK-TAB1 signaling inhibits cell-cycle progression at the G1/S checkpoint. These data suggest that AMPK-TAB1 activated p38 inhibits T cell proliferation by direct inhibition of cyclins, induction of cyclin inhibitors and downstream activation of p53.

p38 activation induces senescence characteristics in non-senescent T cells

To further link the AMPK-TAB1 pathway with p38 spontaneous activation, we activated non-senescent CD27⁺ CD28⁺ CD4⁺ T cells with the AMPK agonist A-769662 either in the presence or absence of the selective p38 inhibitor BIRB 796. A-769662 inhibited the telomerase activity, proliferation and expansion of CD27⁺ CD28⁺ CD4⁺ T cells activated with anti-CD3 and CD28 antibodies, while addition of BIRB 796 restored these functions (Fig. 6a,b and data not shown). Similar results were obtained in p38-silenced CD27⁺ CD28⁺ CD4⁺ T cells (Supplementary Fig. 6a,b). All these observations were reproduced in glucose starved CD27⁺ CD28⁺ CD4⁺ T cells, and they were counteracted in part by p38 inhibition (Supplementary Fig. 6c-e). However, cells did not survive the prolonged absence of glucose after 5 days (data not shown)³⁶. In addition, AMPK activation by the A-769662 agonist induced a dose-dependent loss of TCR signaling molecules in CD27⁺ CD28⁺ CD4⁺ T cells activated with anti-CD3 and CD28 antibodies (Fig. 6c and data not shown), and this was in part prevented by p38 inhibition (Fig. 6d). Taken together, these data show that AMPK inhibits human T cell proliferation and telomerase via activation of p38, a process that requires its allosteric binding to TAB1. Furthermore non-senescent T cells activate p38 and downregulate proliferation and telomerase activity if AMPK is activated chemically or by glucose starvation.

Discussion

In this study we investigated the mechanism of p38 activation in senescent human CD4⁺ T cells. In T cells, p38 activation was previously documented to be induced either by the canonical MAPK cascade or the alternative TCR signaling pathway in response to environmental stress or TCR activation respectively^{10, 11, 19}. Here we have shown that senescent human CD4⁺ T cells lack essential ‘upstream’ components of both the canonical and the alternative pathways and instead activate p38 by a previously unrecognized AMPK-TAB1-dependent mechanism. This occurs *in vivo* in response to endogenous DNA damage response (DDR) signaling by the apical kinase ATM, in response to genotoxic stress. However, glucose starvation can also trigger the energy gauge AMPK and lead to p38 activation via the scaffold TAB1 in non-senescent CD4⁺ T cells that have no DNA damage. Therefore, signaling through this AMPK-TAB1 pathway for p38 activation can be induced in undifferentiated T cells by low nutrient availability or in senescent T cells by DNA damage. This leads to the down-regulation of key signaling molecules of the TCR complex and inhibition of both telomerase activity and proliferation.

The scaffold molecule TAB1 was initially identified as a TAK1 binding partner³⁷. Subsequently, it was found that TAB1 could also induce allosteric p38 auto-phosphorylation in the human embryonic kidney 293 cell line, independently of TAK1^(20, 21). However the biological relevance of TAB1-dependent p38 activation has remained uncertain. In a model of mouse ischemic cardiomyocytes, both TAB1 and AMPK were reported to act upstream of p38⁽²²⁾, but two subsequent studies in the same experimental system challenged the former report^{38, 39}. The reason for the evolution of different modes of P38 MAPK activation are unknown, but our findings suggest that they may enable the same signaling molecule to exert opposite effects on T cell function. For example, we confirmed previous observations that ‘alternative’ DLG-mediated p38 activation downstream of the TCR supports proliferative activity in non-senescent CD4⁺ T cells¹⁷, however, p38 activated via AMPK-TAB1 inhibits proliferation in both senescent and non-senescent human CD4⁺ T cells. Furthermore a recent report showed that ‘canonical’ and ‘alternative’ activated p38 counter-regulate each other in controlling T cell effector functions by exerting different substrate specificity⁴⁰. Also, we note that the mapped TAB1-p38 interaction site⁴¹ impedes access to the ‘alternative’ Y323 regulatory phosphorylation site of p38, suggesting that scaffold molecules may also be involved in the determination of downstream substrate specificity.

One unexpected observation was that key components of the TCR signaling machinery such as LCK, ZAP-70, DLG1, LAT and SLP-76 are naturally lost in senescent CD4⁺ T cells, which also lose CD27 and CD28 expression^(8,35). The collective loss of these signaling molecules will exacerbate the inhibition of proliferation in these cells by decreasing their capacity for TCR activation. Of note, blocking p38 in highly differentiated T cells did not restore expression of the TCR signalosome (data not shown), suggesting that other p38 independent mechanisms are involved.

At present, a number of p38 inhibitors have been developed for use in treating diseases with inflammatory aetiology⁴². When tested in clinical trials, those compounds showed low therapeutic index and engagement of escape or bypass mechanisms, this latter being

possibly due to the regulation of diverse cellular functions by p38 activation⁴². Because inhibition of p38 activity by silencing AMPK or TAB1 *in vitro* enhances human T cell proliferation we suggest the possibility of specific inhibition of this pathway as a strategy for enhancing immune cell function *in vivo*. The crystal structure of the docking site between TAB1 and p38 has been described⁴¹ and is conserved in both the 60-kDA and 50-kDA variants of this molecule²¹. Targeting of this restricted, MKK independent interaction may provide a selective way for dampening p38 activity as it would spare ubiquitous activation by the MAPK cascade¹⁰. One caveat is that the enhancement of telomerase and proliferation in highly differentiated T cells that have evidence of DNA damage may be tumorigenic³⁵. The risk versus possible benefit of selective therapeutic tuning of telomerase in human T lymphocytes *in vivo* remains to be determined.

We have therefore described an ‘intra-sensory’ pathway in T cells that integrates nutrient and DNA damage sensing signals to activate p38. This may be the prototype of a number of convergent signaling pathways linking senescence, immune-modulation, metabolism and cancer. It is possible that AMPK/TAB1 signaling may be involved with p38 activation that is associated in the senescence of different cell types such as fibroblasts and cardiomyocytes in both mice and humans^{43,44} and this requires further study.

Methods

Cells

Heparinized peripheral blood samples were taken from healthy volunteers (aged 40-65, median 52, male 55% and female 45%; n=57). All samples were obtained with the approval of the Ethical Committee of Royal Free and University College Medical School and voluntary informed consent was obtained in accordance with the Declaration of Helsinki. Donors did not have any co-morbidity, were not on any immunosuppressive drugs, and retained physical mobility and lifestyle independence. The CD4⁺ CD27/CD28 defined subsets were isolated from peripheral blood mononuclear cells (PBMC) as previously described¹⁵.

Western Blot analysis

Purified CD4⁺ CD27/CD28 subsets were harvested *ex vivo* immediately after separation. Alternatively, purified human highly differentiated CD4⁺ CD27⁻ CD28⁻ T cells were harvested four days post transduction (see below). Lysates from 2×10^6 cells were obtained and analyzed as previously described³³. Membranes were probed with anti-p38, MKK3, MKK6, phospho-MKK3/6 (Ser¹⁸⁹/Ser²⁰⁷; 22A8), Lck, Zap70 (99F2), TAB1 (C25E9), TAK1, TRAF6 (D21G3), phospho-AMPK α (Thr¹⁷²), AMPK α , phospho- γ H2A-x (Ser¹³⁹), Lat, SLP-76, PLC- γ 1, GAPDH (14C10) all from Cell Signalling. Anti-phospho-p38 (Tyr³²³) was from ECM-Biosciences. hTERT (H-231) and DLG1 (SAP-97, 2D11) antibodies were from Santa Cruz Biotechnology. All immunoblots were developed using the ECL Prime Western Blotting Detection Kit (GE Healthcare), according to the manufacturer’s instructions.

Immunoprecipitation

For co-immunoprecipitation analysis, cell-lysates were prepared using ice-cold HNGT buffer (50 mM HEPES, pH 7.5, 150 mM EDTA, 10 mM sodium pyrophosphate, 100 mM sodium orthovanadate, 100 mM sodium fluoride, 10 mg/ml aprotinin, 10 mg/ml leupeptin, and 1 mM phenylmethylsulfonyl fluoride). Lysates from 20×10^6 purified primary human CD4⁺ CD27⁺ CD28⁺ T cells were incubated with monoclonal antibody to TAB1 or p38 (Cell Signalling) at 4 °C on a rotary shaker overnight. For the minor CD4⁺ CD28⁻ CD27⁻ subset, cells from two separate individuals were pooled to obtain sufficient cells for analysis. Extracts were then incubated with protein A–G conjugated agarose beads (Santa Cruz Biotechnology) at 4 °C for 3 h. Samples were washed and analyzed by western blotting as indicated. Co-immunoprecipitated proteins were detected using Mouse Anti-rabbit IgG Conformation Specific (L27A9; Cell Signalling) or Mouse Anti-rabbit IgG light chain, followed by a secondary anti-mouse IgG antibody (all from Cell Signalling) and ECL Prime Western detection kit (GE Healthcare).

In vitro kinase assay

TAB1 or p38 immunoprecipitates were obtained as above described. Samples were washed twice in lysis buffer and twice in kinase buffer (all from Cell Signaling). Kinase reactions were incubated for 30 min at 30 °C in the presence or absence of 200 μM ATP (Cell Signaling). In some experiments the ATP competitor p38 inhibitor SB-203580 (10 μM) was added directly to the *in vitro* kinase reaction, as indicated. Total p38 and phosphorylated p38 (Thr180-Tyr182) levels were detected using the PhosphoTracer ELISA Kit according to the manufacturer's instructions (Abcam). *In vitro* kinase assays are shown as proportional to fold increase at 450 nm absorbance emission of triplicate wells ± s.e.m.

Detection of intracellular ROS levels and calcium flux

Following surface staining for CD27 and CD28 receptors, human CD4⁺ T cells were incubated for intracellular ROS or Calcium levels with either Dihydroethidium (DHE) or Fluo-4 AM respectively, according to the manufacturer's instructions (Invitrogen Molecular Probes). Cells were analyzed by flow-cytometry using an LSR Fortessa (BD Biosciences).

Lentiviral vector design

We generated the pHIV1-SIREN-GFP system used for knockdown of gene expression as follows. The pSIN-GFP lentivector⁴⁵ was digested with *EcoRI* and *BamHI*, and the PGK promoter was amplified by polymerase chain reaction (PCR) introducing *EcoRI-BamHI* restriction sites. Then, the SFFV promoter from pSIN-GFP plasmid was replaced with the PGK promoter, cloned by blunt-ligation, to generate the pSIN-PGKp-GFP plasmid. This vector was used as a backbone. A cassette containing the human U6 promoter was cloned in this backbone downstream the cPPT sequence between *Clal-EcoRI* restriction sites (see extended vector map, Fig. S2A). A *BamHI* site was introduced downstream of the U6 promoter to clone the shRNAs of interest between *BamHI* and *EcoRI* restriction sites. The U6-shRNA cassette was placed upstream the PGK promoter and GFP. All constructs were engineered by standard cloning techniques.

The following siRNA sequences were used for gene knockdowns: CCTAAGGTTAAGTCGCCCTCG (shCTRL), GGCGGTCCTTCTCAACAACAAG (shTAB1) and ATGATGTCAGATGGTGAATTT (shAMPK α) as described previously^{21,46,47}. The siRNA sequence used for TAB1 knock-down targets a region which is common to both the 60 and 50 kDa isoforms of this molecule. The siRNA target used for p38 knockdown (shP38) was GTACTTCCTGTGTACTCTTTA. VSV-g pseudotyped lentiviral particles, were produced by transient co-transfection of three plasmids in HEK 293 cells as previously described³⁸ and concentrated 100-fold by ultracentrifugation through a 20% sucrose cushion in phosphate-buffered saline (PBS), following re-suspension in PBS containing 10% glycerol. Lentiviral preparations were then titrated for GFP expression using serial dilutions in HEK 293 cells by flow cytometry.

Cell cultures and lentiviral transduction of primary human T lymphocytes

Cells were cultured in RPMI 1640 medium supplemented with 10% heat-inactivated FCS, 100 U/ml penicillin, 100 mg/ml streptomycin, 50 μ g/ml gentamicin, and 2 mM L-glutamine (all from Invitrogen) at 37°C in a humidified 5% CO₂ incubator. Purified human highly differentiated CD4⁺ CD27⁻ CD28⁻ T cells were activated in the presence of plate-bound α CD3 Ab (purified OKT3, 0.5 μ g/ml) plus rhIL-2 (R&D Systems, 10 ng/ml), and then transduced with pHIV1-Siren lentiviral particles (MOI=10) at 48 and 72 hours after activation. For long-term cultures, transduced cells were re-activated every 10 days. Relatively undifferentiated CD4⁺ CD27⁺ CD28⁺ T cells were cultured and transduced as per CD4⁺ CD27⁻ CD28⁻ cells, but cells were activated by plate-bound α CD3 (0.5 μ g/mL) plus α CD28 (0.5 μ g/mL).

Quantitative PCR (Real time analysis)

Four days post transduction, samples from 5×10^5 viable highly differentiated CD4⁺ CD27⁻ CD28⁻ T cells were resuspended in TRIzol (Ambion). For cDNA synthesis, RNA was retro-transcribed using M-MuLV Reverse Transcriptase (New England Biolab) and random primers. P38, AMPK α , TAB1 and hTERT expression was detected by qPCR. Relative transcript expression was normalized against housekeeping GAPDH using the CT threshold cycle method according to the supplier's protocol (Applied Biosystems).

Signaling studies

Briefly, cells were fixed with warm Cytofix Buffer (BD Biosciences) at 37°C for 10 min. Cells were then permeabilized with ice-cold Perm Buffer III (BD Biosciences) at 4°C for 30 min and incubated with antibodies to phospho-p38 (PE; Thr¹⁸⁰/Tyr¹⁸²), γ -H2AX (PE; Ser¹³⁹), under-phosphorylated Rb, phosphorylated Rb (Ser807/Ser811) (all from BD Biosciences) or phospho-AMPK α (Thr¹⁷²), phospho-ATM (Ser¹⁹²¹), phospho-ATF2 (Thr⁷¹), phospho-p53 (Ser⁴⁶), cyclin D1 and p27 (all from Cell Signaling), for 30 min at room temperature. Primary unconjugated antibodies were subsequently probed with a secondary mouse (or goat) PE-conjugated anti-rabbit IgG (BD Biosciences) for 30' at room temperature, in the dark. Cells were washed in Stain Buffer (BD Pharmingen) and immediately run using an LSR Fortessa (BD Biosciences). In some experiments cells were pre-incubated with the AMPK agonist A-769662 (Tocris Bioscience, 150 μ M, 60'), the ATM inhibitor KU-55933 (Calbiochem, 10 μ M, 60') or PMA (Sigma, 20 ng/mL) before

fixing, as indicated (see text). Data analysis was performed using FlowJo software (Treestar). For signaling studies using transduced cells, events were gated on the GFP⁺ compartment as indicated.

Measurement of telomerase activity

Telomerase activity was determined using the TeloTAGGG telomerase ELISA kit from Roche according to the manufacturer's instructions from extracts of 2×10^3 viable transduced CD4⁺ CD27⁻ CD28⁻ T cells. The absolute numbers of CD4⁺ CD27⁻ CD28⁻ T cells were enumerated by trypan blue (Sigma) and Ki67 analysis, as previously described³³. Telomerase activity is expressed as proportional to fold increase at 450nm absorbance emission of triplicate wells \pm s.e.m.

Assessment of Telomere length

Telomere length of transduced CD27⁻ CD28⁻ CD4⁺ T cells was measured after 30 days of activation in culture, using a modified version of the flow-FISH method that was previously described¹⁵. Telomere length of transduced GFP⁺ CD4⁺ CD27⁻ CD28⁻ T cells is shown as the bp variation (Δ) of GFP⁺ AMPK α or TAB1 silenced cells over an irrelevant scrambled control GFP⁺ CD4⁺ CD27⁻ CD28⁻ population.

Proliferation assays

Four days post transduction, proliferation of activated CD27⁻CD28⁻ or CD27⁺ CD28⁺ CD4⁺ T cells was assessed by overnight probing with [³H] thymidine. Short-term proliferative activity is expressed as fold increase in [³H] thymidine incorporation (cpm) of triplicate wells \pm s.e.m. Alternatively, purified human highly differentiated CD27⁻ CD28⁻ CD4⁺ T cells were immediately stained with CellTrace Violet Cell Proliferation Kit and analyzed by flow cytometry 96 hours post-transduction (day 7), according to the manufacturer's instructions (Invitrogen). In some experiments using early differentiated CD27⁺ CD28⁺ CD4⁺ T cells, proliferation was assessed by staining for the cell cycle related nuclear antigen Ki67 following 48 hour activation, as described previously³². Population doubling levels (PDLs) were calculated as \log_{10} (number of cells counted after expansion) – \log_{10} (number of cells seeded)/ $\log_{10} 2$.

Statistical analysis

Graphpad Prism was used to perform statistical analysis. For pairwise comparisons, a paired Student's t test was used. For three matched groups, a one-way analysis of variance (ANOVA) for repeated measures using a Bonferroni posttest correction was used. Differences were considered significant when P was < 0.05 .

Supplementary Material

Refer to Web version on PubMed Central for supplementary material.

Acknowledgements

We thank Sara Sofia Marelli for discussion and revision of the manuscript.

This work was supported by funds from the Medical Research Council (to A.L.) and the Biotechnology and Biological Science Research Council (to A.N.A.). D.E. is funded by a Miguel Servet Fellowship from the Instituto de Salud Carlos III, Spain.

References

1. Huang Y, Wange RL. T cell receptor signaling: beyond complex complexes. *The Journal of biological chemistry*. 2004; 279:28827–28830. [PubMed: 15084594]
2. Akbar AN, Beverley PC, Salmon M. Will telomere erosion lead to a loss of T-cell memory? *Nature reviews. Immunology*. 2004; 4:737–743.
3. Fletcher JM, et al. Cytomegalovirus-specific CD4+ T cells in healthy carriers are continuously driven to replicative exhaustion. *J Immunol*. 2005; 175:8218–8225. [PubMed: 16339561]
4. Henson SM, et al. KLRG1 signaling induces defective Akt (ser473) phosphorylation and proliferative dysfunction of highly differentiated CD8+ T cells. *Blood*. 2009; 113:6619–6628. [PubMed: 19406987]
5. Libri V, et al. Cytomegalovirus infection induces the accumulation of short-lived, multifunctional CD4+CD45RA+CD27+ T cells: the potential involvement of interleukin-7 in this process. *Immunology*. 2011; 132:326–339. [PubMed: 21214539]
6. Warrington KJ, Vallejo AN, Weyand CM, Goronzy JJ. CD28 loss in senescent CD4+ T cells: reversal by interleukin-12 stimulation. *Blood*. 2003; 101:3543–3549. [PubMed: 12506015]
7. Vallejo AN. CD28 extinction in human T cells: altered functions and the program of T-cell senescence. *Immunological reviews*. 2005; 205:158–169. [PubMed: 15882352]
8. Weng NP, Akbar AN, Goronzy J. CD28(-) T cells: their role in the age-associated decline of immune function. *Trends Immunol*. 2009; 30:306–312. [PubMed: 19540809]
9. Di Mitri D, et al. Reversible senescence in human CD4+CD45RA+CD27-memory T cells. *J Immunol*. 2011; 187:2093–2100. [PubMed: 21788446]
10. Ashwell JD. The many paths to p38 mitogen-activated protein kinase activation in the immune system. *Nature reviews. Immunology*. 2006; 6:532–540.
11. Rudd CE. MAPK p38: alternative and nonstressful in T cells. *Nature immunology*. 2005; 6:368–370. [PubMed: 15785766]
12. Chang L, Karin M. Mammalian MAP kinase signalling cascades. *Nature*. 2001; 410:37–40. [PubMed: 11242034]
13. Dodeller F, Schulze-Koops H. The p38 mitogen-activated protein kinase signaling cascade in CD4 T cells. *Arthritis research and therapy*. 2006; 8:205. [PubMed: 16542479]
14. Salvador JM, et al. Alternative p38 activation pathway mediated by T cell receptor-proximal tyrosine kinases. *Nature immunology*. 2005; 6:390–395. [PubMed: 15735648]
15. Plunkett FJ, et al. The loss of telomerase activity in highly differentiated CD8+CD28-CD27- T cells is associated with decreased Akt (Ser473) phosphorylation. *J Immunol*. 2007; 178:7710–7719. [PubMed: 17548608]
16. Yan M, et al. Activation of stress-activated protein kinase by MEKK1 phosphorylation of its activator SEK1. *Nature*. 1994; 372:798–800. [PubMed: 7997270]
17. Jirmanova L, Sarma DN, Jankovic D, Mittelstadt PR, Ashwell JD. Genetic disruption of p38alpha Tyr323 phosphorylation prevents T-cell receptor-mediated p38alpha activation and impairs interferon-gamma production. *Blood*. 2009; 113:2229–2237. [PubMed: 19011223]
18. Round JL, et al. Scaffold protein Dlg1 coordinates alternative p38 kinase activation, directing T cell receptor signals toward NFAT but not NF-kappaB transcription factors. *Nature immunology*. 2007; 8:154–161. [PubMed: 17187070]
19. Rincon M, Davis RJ. Choreography of MAGUKs during T cell activation. *Nature immunology*. 2007; 8:126–127. [PubMed: 17242684]
20. Ge B, et al. MAPKK-independent activation of p38alpha mediated by TAB1-dependent autophosphorylation of p38alpha. *Science*. 2002; 295:1291–1294. [PubMed: 11847341]
21. Ge B, et al. TAB1beta (transforming growth factor-beta-activated protein kinase 1-binding protein 1beta), a novel splicing variant of TAB1 that interacts with p38alpha but not TAK1. *The Journal of biological chemistry*. 2003; 278:2286–2293. [PubMed: 12429732]

22. Li J, Miller EJ, Ninomiya-Tsuji J, Russell RR 3rd, Young LH. AMP-activated protein kinase activates p38 mitogen-activated protein kinase by increasing recruitment of p38 MAPK to TAB1 in the ischemic heart. *Circ Res.* 2005; 97:872–879. [PubMed: 16179588]
23. Hardie DG. AMP-activated protein kinase: an energy sensor that regulates all aspects of cell function. *Genes Dev.* 2011; 25:1895–1908. [PubMed: 21937710]
24. Rolf J, et al. AMPKalpha1: a glucose sensor that controls CD8 T-cell memory. *Eur J Immunol.* 2013; 43:889–896. [PubMed: 23310952]
25. Finlay D, Cantrell DA. Metabolism, migration and memory in cytotoxic T cells. *Nature reviews. Immunology.* 2011; 11:109–117.
26. Sanders MJ, et al. Defining the mechanism of activation of AMP-activated protein kinase by the small molecule A-769662, a member of the thienopyridone family. *The Journal of biological chemistry.* 2007; 282:32539–32548. [PubMed: 17728241]
27. d'Adda di Fagagna F. Living on a break: cellular senescence as a DNA-damage response. *Nat Rev Cancer.* 2008; 8:512–522. [PubMed: 18574463]
28. Mondal AM, et al. p53 isoforms regulate aging- and tumor-associated replicative senescence in T lymphocytes. *The Journal of clinical investigation.* 2013; 123:5247–5257. [PubMed: 24231352]
29. Passos JF, Von Zglinicki T. Oxygen free radicals in cell senescence: are they signal transducers? *Free radical research.* 2006; 40:1277–1283. [PubMed: 17090417]
30. Blattler SM, Rencurel F, Kaufmann MR, Meyer UA. In the regulation of cytochrome P450 genes, phenobarbital targets LKB1 for necessary activation of AMP-activated protein kinase. *Proceedings of the National Academy of Sciences of the United States of America.* 2007; 104:1045–1050. [PubMed: 17213310]
31. Hodes RJ, Hathcock KS, Weng NP. Telomeres in T and B cells. *Nature reviews. Immunology.* 2002; 2:699–706.
32. Reed JR, et al. Telomere erosion in memory T cells induced by telomerase inhibition at the site of antigenic challenge in vivo. *The Journal of experimental medicine.* 2004; 199:1433–1443. [PubMed: 15148341]
33. Lanna A, et al. IFN-alpha Inhibits Telomerase in Human CD8+ T Cells by Both hTERT Downregulation and Induction of p38 MAPK Signalling. *J Immunol.* 2013
34. Akbar AN, Vukmanovic-Stejic M. Telomerase in T lymphocytes: use it and lose it? *J Immunol.* 2007; 178:6689–6694. [PubMed: 17513711]
35. Akbar AN, Henson SM. Are senescence and exhaustion intertwined or unrelated processes that compromise immunity? *Nature reviews. Immunology.* 2011; 11:289–295.
36. Chang CH, et al. Posttranscriptional control of T cell effector function by aerobic glycolysis. *Cell.* 2013; 153:1239–1251. [PubMed: 23746840]
37. Shibuya H, et al. TAB1: an activator of the TAK1 MAPKKK in TGF-beta signal transduction. *Science.* 1996; 272:1179–1182. [PubMed: 8638164]
38. Jacquet S, et al. The relationship between p38 mitogen-activated protein kinase and AMP-activated protein kinase during myocardial ischemia. *Cardiovasc Res.* 2007; 76:465–472. [PubMed: 17765884]
39. Jaswal JS, Gandhi M, Finegan BA, Dyck JR, Clanachan AS. p38 mitogen-activated protein kinase mediates adenosine-induced alterations in myocardial glucose utilization via 5'-AMP-activated protein kinase. *Am J Physiol Heart Circ Physiol.* 2007; 292:H1978–1985. [PubMed: 17172269]
40. Alam SM, Gaida MM, Ogawa Y, Kolios AGA, Lasitschka F, Ashwell JD. Counter-regulation of T cell effector function by differentially activated p38. *The Journal of experimental medicine.* 2014; 211:1257–1270. [PubMed: 24863062]
41. De Nicola GF, et al. Mechanism and consequence of the autoactivation of p38alpha mitogen-activated protein kinase promoted by TAB1. *Nature structural and molecular biology.* 2013; 20:1182–1190.
42. Lee JC, et al. Inhibition of p38 MAP kinase as a therapeutic strategy. *Immunopharmacology.* 2000; 47:185–201. [PubMed: 10878289]
43. Tivey HS, Brook AJ, Rokicki MJ, Kipling D, Davis T. p38 (MAPK) stress signalling in replicative senescence in fibroblasts from progeroid and genomic instability syndromes. *Biogerontology.* 2013; 14:47–62. [PubMed: 23112078]

44. Bernet JD, Doles JD, Hall JK, Kelly Tanaka K, Carter TA, Olwin BB. p38 MAPK signaling underlies a cell-autonomous loss of stem cell self-renewal in skeletal muscle of aged mice. *Nature Medicine*. 2014; 20:265–271.
45. Escors D, et al. Targeting dendritic cell signaling to regulate the response to immunization. *Blood*. 2008; 111:3050–3061. [PubMed: 18180378]
46. Tangeman L, Wyatt CN, Brown TL. Knockdown of AMP-activated protein kinase alpha 1 and alpha 2 catalytic subunits. *J RNAi Gene Silencing*. 2012; 8:470–478. [PubMed: 23316259]
47. Sarbassov DD, Guertin DA, Ali SM, Sabatini DM. Phosphorylation and regulation of Akt/PKB by the rictor-mTOR complex. *Science*. 2005; 307:1098–1101. [PubMed: 15718470]

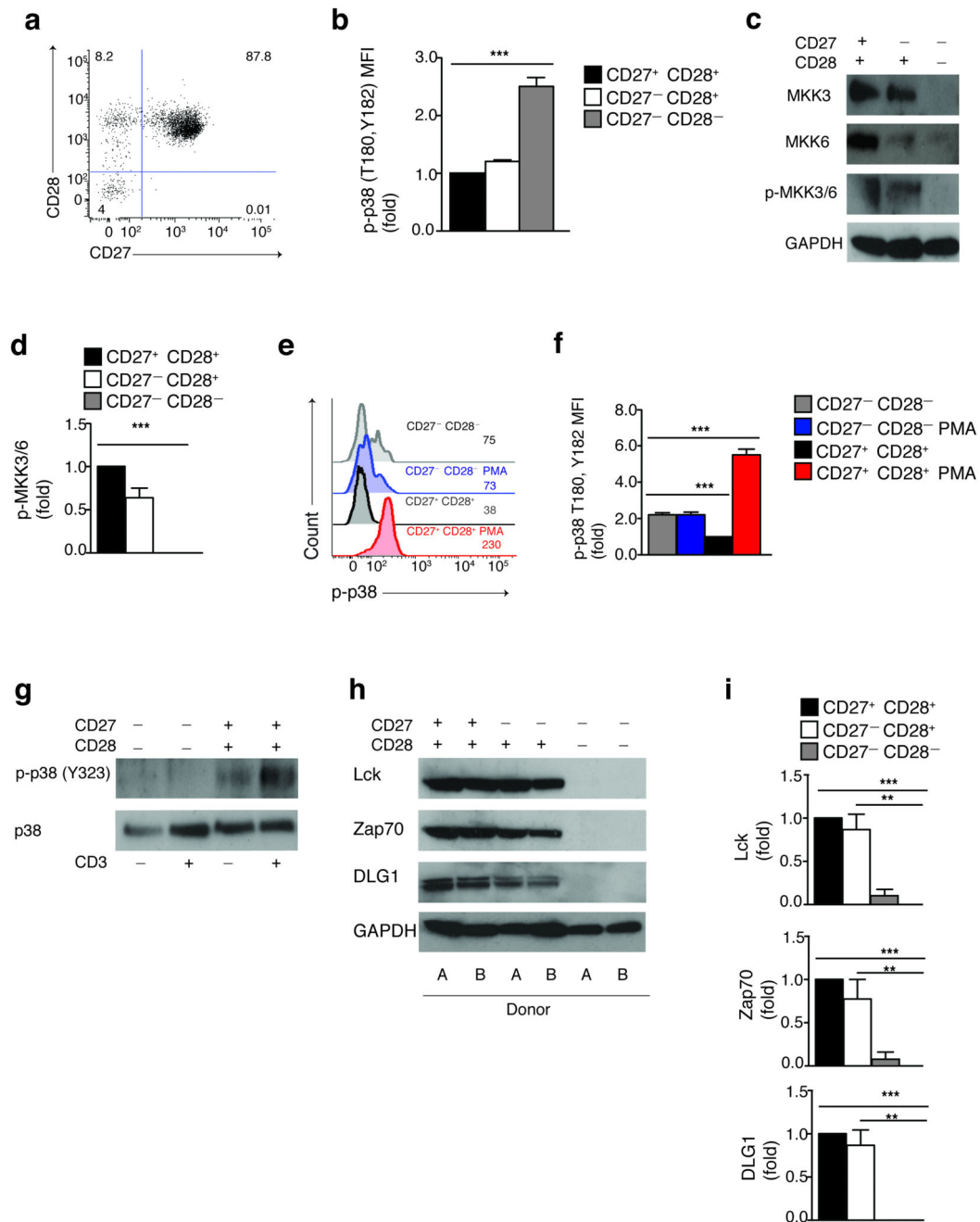


Figure 1. Spontaneous p38 activation in the absence of both upstream canonical and alternative pathways in highly differentiated T cells

(a) The co-expression of CD27 and CD28 receptors by human CD4⁺ T cells, representative staining (n=9). (b) Phospho-flow data of spontaneous p38 (Thr¹⁸⁰, Tyr¹⁸²) phosphorylation in CD4⁺ CD27/CD28 defined subsets from 9 different donors (MFI, mean fluorescence intensity). (c) Immunoblots of total MKK3, MKK6 and phospho-MKK3/MKK6 (Ser¹⁸⁹, Ser²⁰⁶) in CD4⁺ CD27/CD28 defined subsets. GAPDH was used as a loading control. Data are representative of 4 independent experiments. (d) The relative level of

endogenous MKK3/6 activation vs. total GAPDH in CD4⁺ CD27/CD28 defined subsets of 4 separate individuals. **(e)** Representative overlay and **(f)** pooled phospho-flow data from 3 independent experiments showing p38 (Thr¹⁸⁰, Tyr¹⁸²) phosphorylation in CD27⁻ CD28⁻ and CD27⁺ CD28⁺ CD4⁺ T cells either before or after treatment with PMA (20 ng/mL, 60'). **(g)** Immunoblots of total p38 and phospho-p38 (Tyr³²³) in isolated CD27⁻ CD28⁻ and CD27⁺ CD28⁺ CD4⁺ T cells either before or after αCD3 activation (10 μg/mL, 30'). Data are representative of 3 independent experiments. **(h)** Representative blots of total Lck, Zap70 and DLG1 expression in CD4⁺ CD27/CD28 defined subsets; GAPDH was used as a loading control. Two different donors from the same gel are shown. **(i)** The relative level of Lck, Zap70 and DLG1 protein expression vs. total GAPDH in CD4⁺ CD27/CD28 defined subsets of 4 different subjects. All **p* < 0.05, ***p* < 0.01, and ****p* < 0.001 values were calculated using one-way analysis of variance (ANOVA) for repeated-measures with a Bonferroni post-test correction. Error bars depict s.e.m.

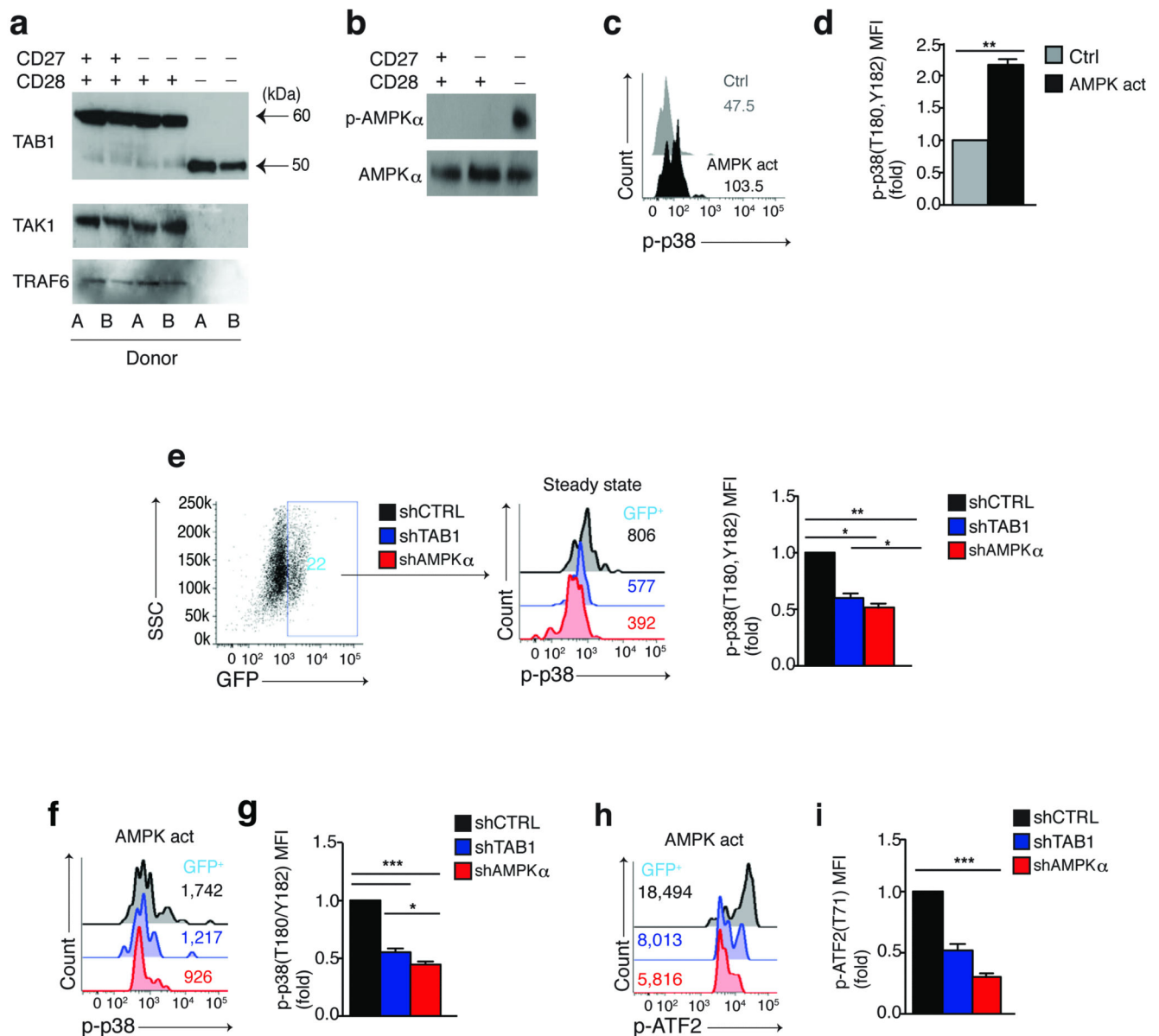


Figure 2. Spontaneous p38 activation triggered by AMPK and mediated by TAB1 in highly differentiated T cells

(a) Immunoblots of TAB1 (alternative isoforms depicted by black arrows), TAK1 and TRAF6 expression from 2 different subjects within the same gel and (b) total AMPK α and phospho-AMPK α (Thr¹⁷²) expression in freshly isolated CD4⁺ CD27/CD28 defined subsets. Data are representative of (a) 4 or (b) 3 different donors. (c) Representative overlay and (d) pooled data from 3 separate experiments showing the effect of the AMPK activator A-769662 (150 μ M, 60') on p38 (Thr¹⁸⁰, Tyr¹⁸²) phosphorylation in CD27⁺ CD28⁺ CD4⁺ T cells as determined by phospho-flow analysis. (e) Representative FACS plot (n=9) showing expression of the reporter GFP gene in transduced purified CD27⁻CD28⁻ CD4⁺ T cells, 96 hours post transduction (*left*); overlay from the same experiment (*middle*) and pooled phospho-flow data from 3 separate experiments (*right*) showing steady-state p38

(Thr¹⁸⁰, Tyr¹⁸²) phosphorylation within the reporter GFP⁺ populations of CD27⁻CD28⁻CD4⁺ T cells transduced with lentiviral vectors encoding either shAMPK α , shTAB1 or shCtrl (knock-down validation in Supplementary Fig. 2). **(f)** Representative overlay and **(g)** pooled data from 3 separate experiments showing the effect of the AMPK activator A-769662 (150 μ M, 60') on p38 (Thr¹⁸⁰, Tyr¹⁸²) phosphorylation in CD27⁻ CD28⁻ CD4⁺ T cells transduced as indicated and analyzed within the GFP⁺ subsets by phospho-flow. **(h)** Representative overlay and **(i)** pooled phospho-flow data of ATF2 (Thr⁷¹) phosphorylation from 3 separate experiments performed as described in (f,g). In **(d)** a paired Student's t test was used. For all other statistics a one-way analysis of variance (ANOVA) for repeated-measures with a Bonferroni post-test correction. $p < 0,05$, $**p < 0,01$, and $***p < 0,001$. Error bars depict s.e.m.

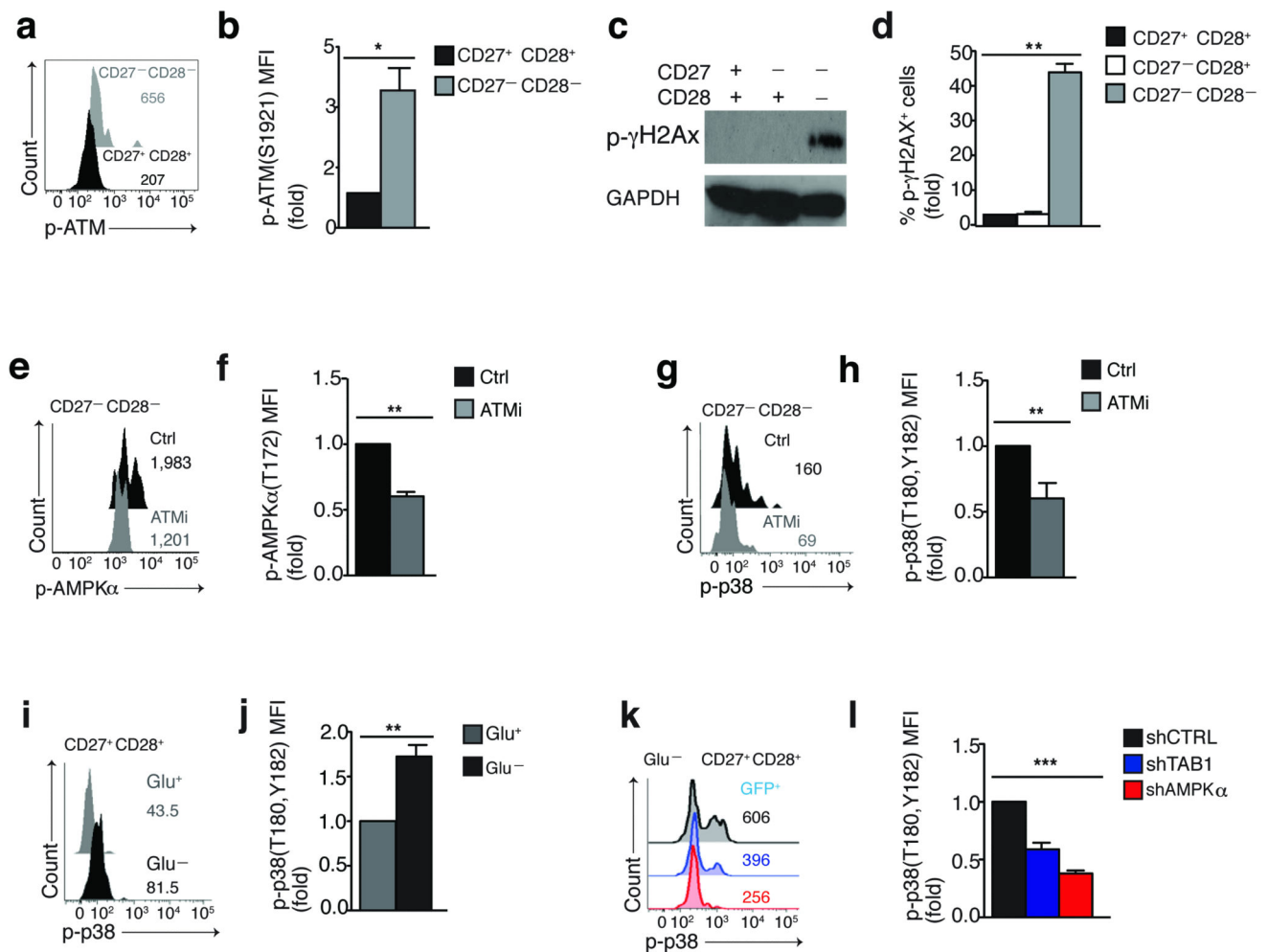


Figure 3. DNA damage and low-nutrient signals converge at AMPK which drives TAB1 dependent p38 activation in T cells

(a) Representative overlay and (b) pooled phospho-flow data from 4 different subjects of spontaneous ATM (Ser¹⁹²¹) phosphorylation in CD27⁻CD28⁻ and CD27⁺CD28⁺ CD4⁺ T cells, directly *ex vivo*. (c) Immunoblot and (d) pooled phospho-flow data from 4 different subjects of γ H2AX (Ser¹³⁹) phosphorylation in freshly isolated CD4⁺ CD27/CD28 defined subsets; GAPDH served as loading control in (c). Immunoblot is representative of 2 independent experiments. (e) Representative overlay and (f) pooled phospho-flow data showing the effect of the selective ATM inhibitor KU-55933 (60', 10 μ M) on constitutive AMPK α (Thr¹⁷²) phosphorylation in CD27⁻CD28⁻ CD4⁺ T cells. (g) Representative overlay and (h) pooled phospho-flow data of p38 (Thr¹⁸⁰, Tyr¹⁸²) phosphorylation from 3 separate experiments performed as described in (e,f). (i) Representative overlay and (j) pooled results from 3 separate experiments showing the effect of 18 hours of glucose starvation on p38 (Thr¹⁸⁰, Tyr¹⁸²) phosphorylation in CD27⁺CD28⁺ CD4⁺ T cells. (k) Representative overlay and (l) pooled data showing the effect of 18 hours glucose starvation on p38 (Thr¹⁸⁰, Tyr¹⁸²) phosphorylation in CD27⁺CD28⁺ CD4⁺ T cells transduced as indicated and analyzed within the GFP⁺ subsets by phospho-flow.

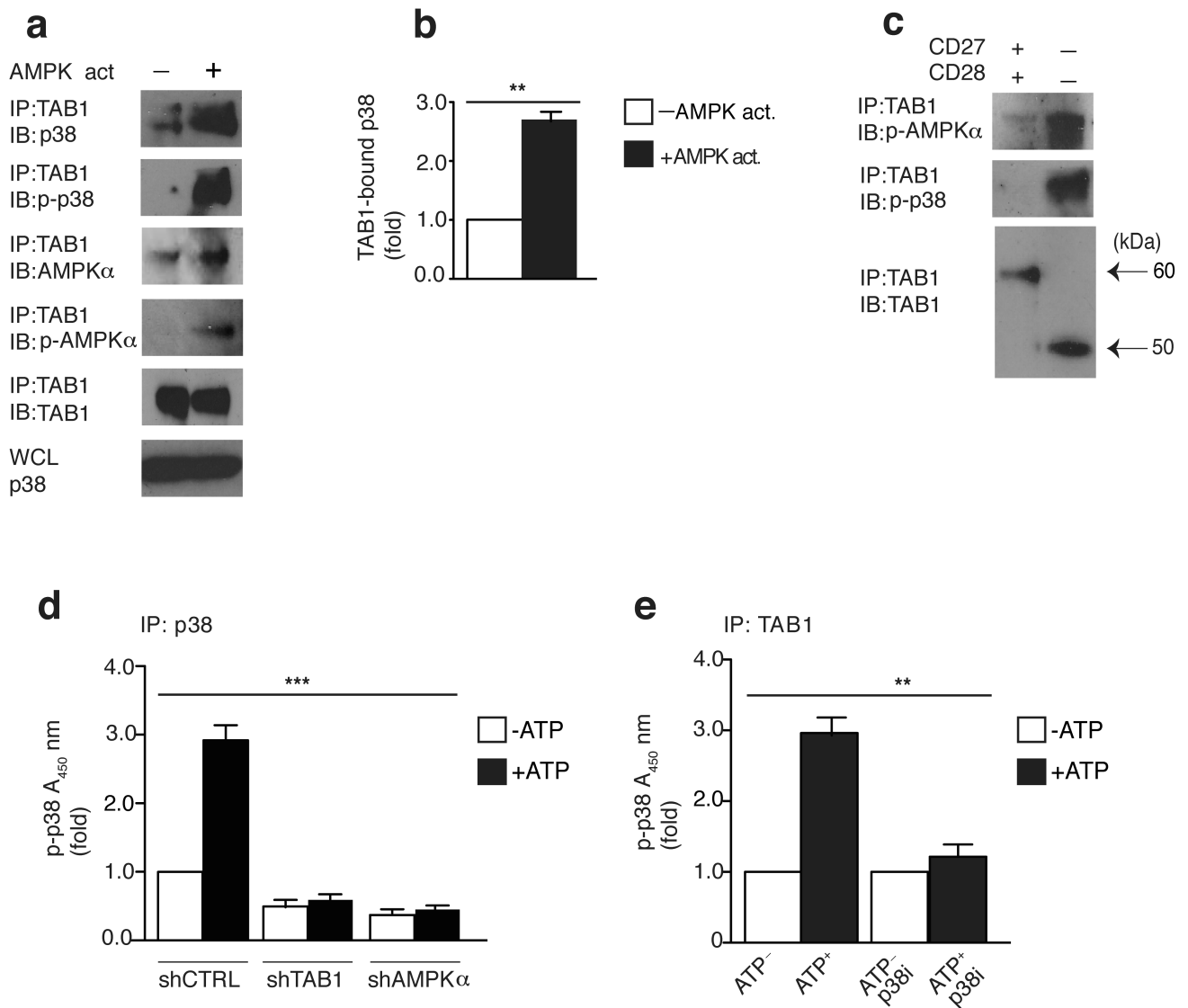


Figure 4. AMPK triggered p38 recruitment to TAB1 causes p38 auto-phosphorylation
(a) Immunoblots of total p38, phospho-p38 (Thr180,Tyr182), total AMPK α phospho-AMPK α (Thr172) and TAB1 in CD27⁺ CD28⁺ CD4⁺ T cells activated with DMSO control or the AMPK agonist A-769662 (150 μ M) for 2 hours, followed by immunoprecipitation with anti-TAB1. Data are representative of 4 separate donors. Immunoblot of total p38 from whole cell lysate (WCL) served as input control. **(b)** The relative binding of p38 to TAB1 upon AMPK activation as determined by 4 independent experiments performed as described in (a). **(c)** Freshly-isolated CD27⁺ CD28⁺ or CD27⁻ CD28⁻ CD4⁺ T cells were immunoprecipitated with anti-TAB1 and analyzed by immunoblot, as indicated (alternative TAB1 isoforms depicted by black arrows). Data are representative of 2 separate experiments (for the minor CD4⁺ CD27⁻ CD28⁻ T cell fraction, cells were pooled together from 2 different donors to achieve sufficient cell number to perform the assay). **(d)** Measurement of p38 auto-phosphorylation by ELISA-based *in vitro* kinase assay of p38 immunoprecipitates from transduced purified CD27⁺ CD28⁺ CD4⁺ T cells reactivated with the AMPK agonist

A-769662 (150 μM) for 2 hours. Immunoprecipitates were left untreated or incubated for 30 min with ATP (200 μM). (e) Measurement of p38 auto-phosphorylation of TAB1 immunoprecipitates from $\text{CD4}^+ \text{CD27}^+ \text{CD28}^+$ T cells activated with the AMPK agonist A-769662 (150 μM) for 2 hours. The assay was performed as described in (d) in the presence or absence of the p38 inhibitor SB-203580 (10 μM). Experiments in (d,e) were performed from 3 different donors. In (b) a paired Student's t test was used; for (d) and (e) a one-way analysis of variance (ANOVA) for repeated-measures with a Bonferroni post-test correction. * $p < 0,05$, ** $p < 0.01$, and *** $p < 0.001$. Error bars depict s.e.m.

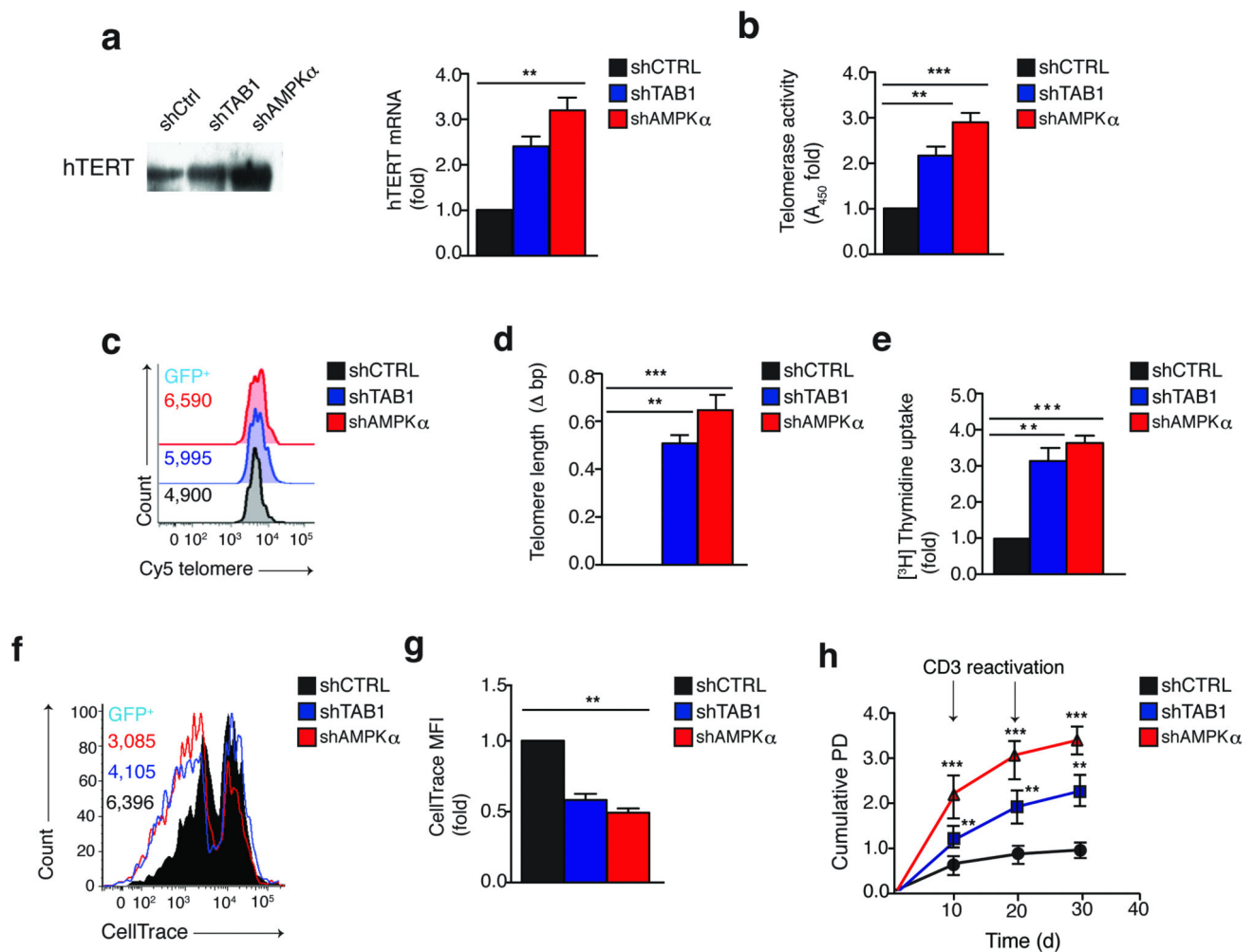


Figure 5. Silencing of AMPK or TAB1 restores telomerase and proliferation in highly differentiated T cells

(a) Measurement of hTERT expression by both immunoblot (left) and quantitative PCR (right) in CD27⁻ CD28⁻ CD4⁺ T cells, transduced as indicated and analyzed 96 hours later (see also Supplementary Fig. 4a). Immunoblot of hTERT expression is representative of 2 independent experiments; samples for quantitative PCR are from 3 different donors and normalized against housekeeping GAPDH expression. (b) Telomerase activity by TRAP assay in CD27⁻ CD28⁻ CD4⁺ T cells transduced and cultured as described in (a). Data are from 3 separate donors. (c) Representative overlay and (d) the pooled flow-fish data from 3 separate experiments showing telomere elongation in both shAMPK α and shTAB1 transduced GFP⁺ CD27⁻ CD28⁻ CD4⁺ T cells vs the shCtrl GFP⁺ population. Telomere length was measured after 2 rounds of activation in culture (day 30; see also Supplementary Fig. 4a). (e-f) Proliferative activity by (e) [³H] thymidine incorporation assay (n=3) or (f) dye dilution analysis in CD27⁻ CD28⁻ CD4⁺ T cells transduced as indicated and analyzed 96 hours later. (g) The pooled results of 3 separate experiments performed as in (f). (h) Replicative lifespan by cumulative PD of long-term cultured CD27⁻ CD28⁻ CD4⁺ T cells, transduced as indicated (see also Supplementary Fig. 4a). Data are from 3 separate donors. All * $p < 0.05$, ** $p < 0.01$, and *** $p < 0.001$ values were calculated using a one-way analysis

of variance (ANOVA) for repeated-measures with a Bonferroni post-test correction. Error bars depict s.e.m.

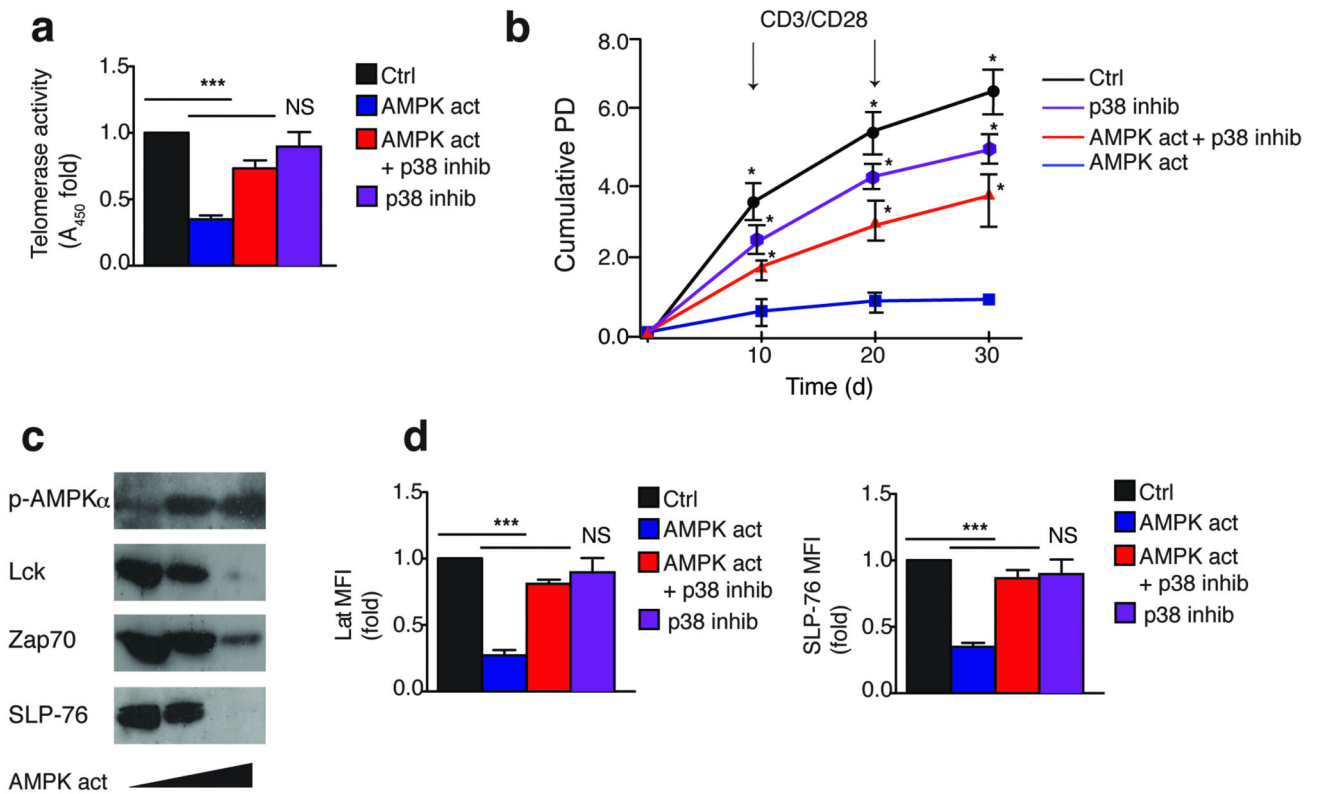


Figure 6. p38 activation by a specific AMPK agonist reproduces senescent features in non-senescent T cells

(a) Telomerase activity by TRAP assay in CD27⁺ CD28⁺ CD4⁺ T cells activated by α CD3/CD28 and cultured as indicated for 3 days. AMPK was activated by A-769662 (150 μ M); p38 was inhibited by BIRB 796 (500 nM). A DMSO vehicle solution was used as control. Experiments are from 3 different donors. (b) Replicative lifespan of long-term cultured CD27⁺ CD28⁺ CD4⁺ T cells assessed by cumulative PD from 3 separate donors. Cells were activated and cultured as described in (a). (c) Immunoblots showing the dose-dependent effect of the AMPK agonist A-769662 (0, 100 or 150 μ M) on total Lck, Zap70 and SLP-76 expression, after 3 days, in CD27⁺ CD28⁺ CD4⁺ T cells activated by α CD3/CD28. A DMSO vehicle solution was used as control; detection of AMPK α ¹⁷² phosphorylation served as pharmacological activation control. Immunoblots are representative of 4 independent experiments. (d) Pooled phospho-flow data from 3 independent experiments showing Lat and SLP-76 expression in CD27⁺ CD28⁺ CD4⁺ T cells cultured as described in (a-b) for 3 days. All $*p < 0.05$, $**p < 0.01$, and $***p < 0.001$ values were calculated using a one-way analysis of variance (ANOVA) for repeated-measures with a Bonferroni post-test correction. Error bars depict s.e.m.